

Calreticulin promotes EMT in pancreatic cancer via mediating Ca²⁺ dependent acute and chronic endoplasmic reticulum stress

Weiwei Sheng

China Medical University First Hospital

Guosen Wang

First Affiliated Hospital of Nanchang University

Jingtong Tang

China Medical University First Hospital

Xiaoyang Shi

China Medical University First Hospital

Rongxian Cao

People's Hospital of Liaoning Province

Jian Sun

China Medical University First Hospital

YiHeng Lin

China Medical University First Hospital

Chao Jia

China Medical University First Hospital

Chuanping Chen

the Sixth Peoples' hospital of Shenyang

Jianping Zhou

China Medical University First Hospital

Ming Dong (✉ dongming@cmu.edu.cn)

The first hospital of China Medical University <https://orcid.org/0000-0003-2685-1420>

Research

Keywords: Calreticulin, Intracellular free Ca²⁺, Endoplasmic reticulum stress, IRE1 α , Epithelial mesenchymal transition, Pancreatic cancer

Posted Date: September 4th, 2020

DOI: <https://doi.org/10.21203/rs.3.rs-36928/v2>

License:  This work is licensed under a Creative Commons Attribution 4.0 International License. [Read Full License](#)

Version of Record: A version of this preprint was published on October 7th, 2020. See the published version at <https://doi.org/10.1186/s13046-020-01702-y>.

Abstract

Background: Our previous study showed that calreticulin (CRT) promoted EGF-induced epithelial-mesenchymal transition (EMT) in pancreatic cancer (PC) via Integrin/EGFR-ERK/MAPK signaling. We next investigated the novel signal pathway and molecular mechanism involving the oncogenic role of CRT in PC.

Methods: We investigated the potential role and mechanism of CRT in regulating intracellular free Ca^{2+} dependent acute and chronic endoplasmic reticulum stress (ERS)-induced EMT in PC in vitro and vivo.

Results: Thapsigargin (TG) induced acute ERS via increasing intracellular free Ca^{2+} in PC cells, which was reversed by CRT silencing. Additionally, CRT silencing inhibited TG-induced EMT in vitro by reversing TG-induced changes of the key proteins in EMT signaling (ZO-1, E-cadherin and Slug) and ERK/MAPK signaling (pERK). TG-promoted cell invasion and migration was also rescued by CRT silencing but enhanced by IRE1 α silencing (one of the key stressors in unfolded protein response). Meanwhile, CRT was co-immunoprecipitated and co-localized with IRE1 α in vitro and its silencing led to the chronic ERS via upregulating IRE1 α independent of IRE1-XBP1 axis. Moreover, CRT silencing inhibited IRE1 α silencing-promoted EMT, including inhibiting the activation of EMT and ERK/MAPK signaling and the promotion of cell mobility. In vivo, CRT silencing decreased subcutaneous tumor size and distant liver metastasis following with the increase of IRE1 α expression. A negative relationship between CRT and IRE1 α was also observed in clinical PC samples, which coordinately promoted the advanced clinical stages and poor prognosis of PC patients.

Conclusions: CRT promotes EMT in PC via mediating intracellular free Ca^{2+} dependent TG-induced acute ERS and IRE1 α -mediated chronic ERS via Slug and ERK/MAPK signaling.

Background

Pancreatic cancer (PC) is one of the most aggressive and lethal cancers, with an estimated 55,440 new cases and 44,330 deaths in United States in 2018¹. The strong ability of local invasion and rapid metastasize are major hallmarks of PC, which contribute to the poor prognosis of patients. Thus, it is urgent to reveal the molecular mechanisms and target therapies toward the malignant biology and aggressive progression in PC.

Calreticulin (CRT), as a highly conserved endoplasmic reticulum (ER) Ca^{2+} -buffering chaperone, involves in various cellular processes². We previously reported that CRT overexpression promoted cell invasion, migration and drug resistance of PC by activating ERK/MAPK pathway³. Most recently, we showed that CRT silencing inhibited EGF-induced epithelial-mesenchymal transition (EMT) via the Integrin/EGFR-ERK/MAPK pathway in PC⁴. Based on previous studies, we next investigated the novel signaling pathways and molecular mechanisms involving the oncogenic role of CRT in PC development.

Endoplasmic reticulum stress (ERS) is a defensive response induced by various pathophysiological factors, which is triggered by three transmembrane signal transducers from unfolded protein response (UPR) family: PKR-like endoplasmic reticulum kinase (PERK), inositol-requiring enzyme 1 α (IRE1 α) and activating transcription factor-6 (ATF-6)⁵. ERS plays a significant role in tumor biology including EMT mediated tumor invasion and metastasis⁶. However, the definite role of ERS in malignancies remains controversial⁷. Emerging evidences suggest that ERS plays a dual role in tumor progression. A transient ERS response activates a protective function and pro-survival pathway to cancers, whereas long term ERS triggers death signaling^{8,9}.

Intracellular free Ca^{2+} is a multifunctional second messenger that controls diverse cellular functions¹⁰. Recently, we have reported that alteration of CRT mediates intracellular free Ca^{2+} concentration in PC cells⁴. Moreover, dysfunction of cellular Ca^{2+} homeostasis is a main stimulator of ERS¹¹, which is closely related with cell invasion, immune evasion, EMT and drug

resistance in various cancers¹². Therefore, we sought to evaluate the potential role of CRT in Ca²⁺ homeostasis mediated ERS and EMT in PC, which, to our knowledge, has not been reported yet.

Materials And Methods

Tissue samples and cell lines

This study was approved by the academic committee at the First Hospital of China Medical University. Written informed consent has been obtained from each patient. Eight-one pancreatic ductal adenocarcinoma (PDAC) tissues were procured from surgical resection specimens collected by the Department of Gastrointestinal Surgery at the First Hospital, China Medical University.

Human Capan-2 PC cell line was obtained from the American Type Culture Collection (ATCC, Manassas, VA, USA). SW1990 human PC cell line was purchased from the Cell Bank of the Chinese Academy of Sciences (Shanghai, China). Cells were cultured with recommended growth media with 10% fetal bovine serum (FBS, HyClone, Logan, UT, USA).

Fluo-3 assay

Thapsigargin (TG, Sigma, St Louis, MO, USA) is one of the key stimulators that cause acute ERS via specific inhibiting sarcoplasmic/endoplasmic reticulum Ca²⁺-ATPases (SERCAs), resulting in an increase of cytoplasmic Ca²⁺ concentration¹³. The intracellular free Ca²⁺ concentration was measured using Fluo-3 AM (Beyotime, Shanghai, China), according to the manufacturer's instructions. Briefly, transfected PC cells were pretreated with 200 nM TG and 1% DMSO (control) for 4 h. Cells without or with TG treatment were subsequently loaded with 2 μM Fluo-3 AM for 30 min at 37 °C and then washed with Hanks' Balanced Salt Solution (HBSS, Beyotime) for 3 times. Kept incubating with HBSS for 20 min, the fluorescence was visualized on a confocal microscopy (Leica Tcs Sp5 II, Leica, Heidelberg, Germany) at an excitation wavelength of 488 nm with an emission wavelength of 525 nm.

In addition, cells without or with TG stimuli were harvested by pancreatic enzymes without EDTA, washed by HBSS for 3 times, and then submitted to analysis by flow cytometry. Image analysis was performed using the Image J software. Each experiment was repeated 3 times.

Immunohistochemistry (IHC) assay

As described previously^{4,14}, 4-μm sections were covered with 0.3% H₂O₂, subjected to high pressure, added with goat serum, and then incubated with primary antibodies: CRT (Abcam, Cambridge, UK) and IRE1α (Cell Signaling Technology, CST, Beverly, MA, USA). Then the slices were incubated with the secondary antibodies, treated with streptavidin–peroxidase reagent, visualized with DAB, counterstained with hematoxylin and finally evaluated under microscope. The location of CRT and IRE1α in cytoplasm were considered for scoring. Staining intensity was scored as 0-3 (negative, weak, medium and strong). Extent of staining was scored as 0 (<5%), 1 (5–25%), 2 (26–50%), 3 (51–75%), and 4 (>75%) according to the positive staining areas to the whole carcinoma. The final scores were calculated by 3 pathologists. We used the same scoring method to evaluate the IHC assay in vivo and in human PDAC specimens.

Immunofluorescence (IF) staining

Capan-2 and SW1990 cell lines were implanted into 24-well culture plates covered with slices, fixed in 4% paraformaldehyde, permeabilized with Triton X-100 (0.5%) and incubated with 5% BSA. Then plates were incubated with the primary antibodies overnight: CRT (Abcam) and IRE1 α (Cell signaling technology). The secondary antibodies (Proteintech, Chicago, IL, USA) were conjugated with FITC for CRT and TRITC for IRE1 α . Hoechst33258 were used for nuclear visualizing.

Western blot (WB) assay

Whole protein lysates were prepared from transfected PC cells. Samples were loaded onto 10% SDS-polyacrylamide gels, transferred to PVDF membranes and incubated with primary antibodies: CRT (Abcam), IRE1 α (CST), PREK (CST), phosphorylation PKR-like endoplasmic reticulum kinase (p-PERK, CST), ATF-6 (CST), ZO-1 (Proteintech), ZEB1 (Proteintech), N-cadherin (Proteintech), E-cadherin (Proteintech), Vimentin (Proteintech), phosphorylation extracellular regulated protein kinases (pERK, CST), extracellular regulated protein kinases (ERK, CST), X-box-binding protein 1 (XBP1, Proteintech), Snai1 (Proteintech), Slug (CST), Cavelino-1 (Proteintech), GAPDH (Proteintech) and β -actin (Proteintech) antibodies overnight at 4°C. Then, membranes were incubated with secondary antibodies (Santa Cruz, CA, UK) and finally detected with an ECL detection kit (Thermo Scientific, Rockford, IL, USA). The experiments were repeated for 3 times.

Coimmunoprecipitation (CoIP) assay

CoIP was performed as before^{4,14}. Briefly, PC cells were lysed in lysis buffer and the soluble supernatants were isolated. Magnetic beads (Bio-Rad, California, USA) were preincubated with primary CRT (Abcam), IRE1 α (CST) or IgG (Santa Cruz) antibodies at 4°C for 4 h with rotation. Then antibody-beads complexes were incubated with soluble supernatants at 4°C overnight. Immunoprecipitated proteins were analyzed by WB with a variety of antibody.

CRISPR/Cas9 and siRNA mediated silencing of CRT and IRE1 α

Lentiviruses were synthesized by Genechem (Shanghai, China). PC cells were transfected with lenti-cas9 or lenti-sgRNA as described previously^{4,14}, and then screened using puromycin (Sigma). The stable sub-lines were subsequently transfected with sg1-CRT or sg2-CRT to specifically silence the target gene or an sgRNA control (scramble).

IRE1 α siRNA and siRNA control were synthesized from GenePharma (Shanghai, China). Cells were transiently transfected with siRNA (20 μ M) using oligofectamine3000 (Invitrogen, Carlsbad, CA, USA) as described by the protocol. All target sequences mentioned above were shown in Supplemental Material Table 1.

TG induced EMT construction

Stable transfected PC cells were treated with 200 nM TG or 1% DMSO (as a control) for 4 h. The EMT construction was verified by EMT-enhanced cell invasion and migration and EMT-induced changes in key proteins involving in EMT signaling.

Invasion and migration assays

Briefly, transfected PC cells (pretreated with TG or co-transfected with IRE1 α) were plated in inserts that coated with matrigel (BD Biosciences, Sparks, MD, USA) in 24 well plates with FBS-free growth media. Growth media with 10% FBS was added to

the bottom wells to generate a serum gradient. After 24 h, cells that had migrated to the underside of the inserts were stained with Crystal Violet Hydrate (Sigma). The migratory cells were counted in five random fields per well. The migration assay was done in a similar fashion without matrigel. Each experiment was repeated 3 times.

In vivo xenograft model

All animal work was performed in accordance with protocols approved by the Animal Care Committee of China Medical University. Total 15 nude mice (BALB/c-nu) were used. Transfected Capan-2 cells (1×10^6) were respectively injected into bilateral axillae of 5 nude mice to construct subcutaneous tumor formation. Tumor volumes were calculated by the following formula: length \times width \times height \times 0.52 in cm. Besides, transfected SW1990 cells (1×10^6) were injected into the spleen of 10 nude mice to construct distant liver metastasis model, which were assessed by the number of liver metastases. These nude mice were killed 30 days later, and samples were extracted and fixed for hematoxylin and eosin (HE), and IHC staining.

Statistical analysis

Statistical analysis was performed using SPSS software 21.0 (Chicago, IL, USA). Continuous variables were expressed as the mean \pm SD. The differences in intracellular free Ca^{2+} concentration, WB assay, cell migration and invasion assays and the number of liver metastases were compared through Student's t-test. The differences of orthotopic tumor volumes were compared with paired sample t-test. Non-parametric and spearman correlation tests were analyzed for IHC assays in vivo and human PC samples. The association of target proteins expression with clinicopathological data was analyzed by Chi-squared. The Kaplan-Meier curve was used to estimate survival, and differences were analyzed by the log-rank test. $P < 0.05$ or $P < 0.01$ was considered significant.

Results

CRT silencing inhibited TG-induced increase of intracellular free Ca^{2+} concentration in vitro

Our previous study showed that CRT regulated intracellular free Ca^{2+} in PC cells⁴. Continuing to use the Fluo-3 assay, confocal microscopy showed that TG induced the increase of intracellular free Ca^{2+} in Capan-2 and SW1990 cells, which was significantly inhibited by CRT silencing (Figure 1A and C). Without any stimulus, CRT silencing partially decreased intracellular free Ca^{2+} in PC cells. Upon TG, the growing gap of intracellular free Ca^{2+} between scramble groups with and without TG was much more obvious than that in sg1-CRT and sg2-CRT groups (Figure 1A and C). Similarly, in flow cytometry assays, upon TG, the growing gap of intracellular free Ca^{2+} between scramble groups with and without TG was much more obvious than that in sg1-CRT and sg2-CRT groups (Figure 1B and D). It indicates that the increase of intracellular Ca^{2+} induced by TG is partially regulated by CRT.

CRT silencing inhibited TG-induced EMT in vitro

Intracellular free Ca^{2+} , acts as the second messenger, is essential for multiple cellular functions including invasion and migration¹⁰. Our previous study reasoned that CRT regulated intracellular free Ca^{2+} in PC via Integrin/EGFR-ERK/MAPK, which played an important role in EGF-induced EMT. Ca^{2+} signaling-mediated EMT has also been reported in various cancers^{12,15}. However, the relationship between Ca^{2+} mediated ERS and EMT remains controversial^{16,17}.

TG treatment caused cell apoptosis in various cancers¹⁸. To our surprise, we found an oncogenic role of TG in PC cells via activating acute ERS. Firstly, TG activated EMT and ERK/MAPK signaling by inducing the decrease of EMT epithelial markers E-cadherin and ZO-1, and the increase of pERK and EMT key regulators Snai1, Slug and ZEB1 in Capan-2 and SW1990 cells (Figure 2A, B and Supplemental Figure 1). However, CRT silencing reversed TG-induced the changes of above proteins (except for ZEB1 and Snai1). In detail, without TG stimuli, E-cadherin and ZO-1 expression were slightly increased and pERK and Slug expression was partially decreased in sg-CRT group compared with scramble group. Other EMT markers, such as Snai1, ZEB-1, N-cadherin, Vimentin and Caveolin-1 were unchanged (Figure 2A, B and Supplemental Figure 1). However, upon TG stimuli, a significant increase of E-cadherin and ZO-1 and decrease of pERK and Slug were found in sg-CRT group compared with scramble group in both Capan-2 and SW1990 cells (Figure 2). In addition, TG induced IRE1 α expression in vitro which was one of the key stressors in UPR. Meanwhile, CRT silencing stably upregulated IRE1 α expression whatever with or without TG treatment (Figure 2A, B and Supplemental Figure 1).

For cell mobility assays, TG stimulated cell invasion and migration in both Capan-2 and SW1990 cells (Figure 3). Without TG, CRT silencing alone partially inhibited cell invasion and migration in both two cell lines. However, upon TG, a significant increase of cell invasion and migration were found in scramble groups. Namely, the growing gap of cell motility between scramble groups with and without TG was much more obvious than that in sg1-CRT and sg2-CRT groups (Figure 3). Interestingly, IRE1 α silencing enhanced TG-induced cell invasion and migration in both Capan-2 and SW1990 cells in Supplemental Figure 2. We reasoned that the compensatory increase of IRE1 α induced by TG partially inhibited TG-induced cell mobility in vitro.

Taken together, CRT silencing inhibited TG-induced acute ERS and EMT in vitro via Slug and ERK/MAPK signaling.

CRT silencing upregulated IRE1 α (one of the UPR key stressors) independent of XBP1 in vitro

Chronic ERS produces endogenous or exogenous damage to cells and triggers an evolutionarily conserved response, termed UPR that including three major stressors located on the ER membrane: PERK, IRE1 α and ATF6¹⁹. As mentioned above, CRT silencing led to a stable low level of intracellular Ca²⁺ in PC cells, which contributes to chronic ERS in many cells and tissues^{20,21}. Meanwhile, CRT silencing stably upregulated IRE1 α expression whatever with or without TG treatment. Thus, we next investigated the role of CRT in mediating chronic ERS and EMT in PC. WB showed that CRT silencing upregulated IRE1 α expression in both Capan-2 and SW1990 cells, but had no effect in PERK and ATF6 expression (Figure 2C, D and Supplemental Figure 1). Meanwhile, CRT was co-immunoprecipitated with IRE1 α in the lysates of above cell lines whatever with or without TG treatment (Figure 4A-D). IF further showed the partial co-location of CRT and IRE1 α in vitro (Figure 4E). Thus, a specific interaction between CRT and IRE1 α was observed in CRT-mediated chronic ERS.

IRE1 α acts as an oncogene in prostate cancer and glioblastoma^{22,23}. It is responsible for alternative splicing of the XBP1 transcription which induces Snail expression to promote EMT in breast cancer cells²⁴. Therefore, we next investigated whether CRT mediated chronic ERS-induced EMT via regulating IRE1/XBP1 axis. We first found that IRE1 α protein was much lower in IRE1 α siRNA group compared with control siRNA group, especially in IRE1 α -1 siRNA and IRE1 α -3 siRNA groups (Figure 5A, B and Supplemental Figure 3). To our surprise, IRE1 α silencing promoted EMT in PC cells via Slug and ERK/MAPK signaling. In Capan-2 and SW1990 cells, IRE1 α silencing promoted Slug and pERK expression and inhibited E-cadherin and ZO-1 expression, but had no effect in Snai1, ZEB-1, N-cadherin, Vimentin and Caveolin-1 expression (Figure 5C, D). XBP1, as a spliced target by IRE1 α , was also unchanged. However, CRT silencing reversed IRE1 α siRNA mediated changes in EMT and ERK/MAPK signaling independent of IRE1 α /XBP1 axis (Figure 5C, D). Downregulation of E-cadherin and ZO-1 and upregulation of Slug and pERK were less significant in IRE1 α siRNA plus sg2-CRT group, compared with that in control siRNA plus scramble group (Figure 5C, D). In addition, IRE1 α silencing significantly promoted cell invasion and migration in PC cells, which was also significantly reversed by CRT silencing (Figure 6). In detail, compared with control siRNA plus scramble group, the growing gap of cell motility in IRE1 α siRNA plus scramble group was much more significant

than that in IRE1 α siRNA plus sg2-CRT group (Figure 6). Taken together, CRT silencing inhibited IRE1 α silencing-induced chronic ERS and EMT in vitro via Slug and ERK/MAPK signaling independent of IRE1 α /XBP1 axis.

CRT silencing inhibited subcutaneous tumor size and distant liver metastasis in vivo

Capan-2 cells (derived from primary PC) were used to construct subcutaneous tumorigenesis model in bilateral axillae of the nude mice. Tumor volumes in sg2-CRT group were much smaller than that in paired scramble group (Figure 7A). HE staining confirmed the tumor pathology in both groups (Figure 7B). IHC further verified that CRT expression was significantly decreased but IRE1 α was increased in sg2-CRT group compared with the scramble group, and vice versa (Figure 7B).

SW1990 cells (derived from spleen metastasis) were used to construct liver metastasis model in nude mice. The number of liver metastases in sg2-CRT group were less than that in scramble group (Figure 7C). HE staining also showed a large and serial area of liver metastasis in scramble group compared with that in sg2-CRT group (Figure 7D). IHC further verified that CRT expression was significantly decreased but IRE1 α was increased in sg2-CRT group compared with the scramble group, and vice versa (Figure 7D).

A negative expression between CRT and IRE1 α cooperatively affected the survival of PC patients

Finally, we investigated the close relationship between CRT and IRE1 α with the clinicopathological data of PC patients. CRT was overexpressed (50/81; 61.7%), but IRE1 α was downregulated (38/81; 46.9%) in 81 PC samples (Figure 8A-F). CRT overexpression was positively associated with lymph nodes metastasis and UICC stage (P=0.003 and P=0.004, respectively), while IRE1 α positive expression was negatively associated with lymph nodes metastasis and UICC stage (P=0.012 and P=0.002, respectively) (Table 1). A negative expression between CRT and IRE1 α was also observed in human PC samples (r=-0.278; P=0.012) (Table 2). In serial sections, most PC tissues with high CRT expression trended to be associated with negative IRE1 α expression (Figure 8B, E), and vice versa (Figure 8C, F).

In addition, CRT high expression or IRE1 α positive expression were associated with the poor and better prognosis, respectively (P=0.012; P=0.035, respectively) (Figure 8G and H). Moreover, patients with high CRT and negative IRE1 α expression had a much worse survival (P=0.011) (Figure 8I). Taken together, the close interaction of CRT and IRE1 α coordinately participated in the aggressive clinical stages and prognosis of PC patients.

Discussion

Due to the strong peripancreatic invasion and distant metastasis as well as insensitivity to chemotherapy, the prognosis of PC patients is extremely poor, with a 5-year survival rate of less than 5%²⁵. It is now well recognized that EMT is the "booster" for the malignant progression of PC²⁶, which is implicated in enhancing invasion and metastasis in malignancies. EMT is typically characterized by the activation of ZEB1, N-cadherin, Vimentin, Snai1, Slug and Caveolin-1, and the downregulation of epithelial markers E-cadherin and ZO-1 expression^{27,28}. Our previous study confirmed that CRT silencing inhibited EGF-induced EMT in PC via Integrin/EGFR-ERK/MAPK signaling⁴. In present study, we first demonstrated that CRT mediated EMT via regulating intracellular free Ca²⁺ mediated acute and chronic ERS in PC, which, to our knowledge, has not been reported yet.

CRT, initially identified as a ubiquitous ER protein in 1974²⁹, has diverse biological functions in cellular metabolism and biology, depending on the different locations inside and outside the ER³⁰. CRT regulates Ca²⁺ homeostasis and molecular chaperoning activity within the ER³¹. However, CRT located in the cytoplasm plays contradictory roles in cancer progression³². For example, CRT exhibits an oncogenic role in lung³³, breast^{34,35}, gastric³⁶, hepatic³⁷ and bladder cancers³⁸,

as well as in oral³⁹ and esophageal squamous cell carcinoma^{40,41}, but acts as a tumor suppressor in neuroblastoma^{42,43}. Meanwhile, the role of CRT remains inconclusive in colon⁴⁴⁻⁴⁷, prostate^{48,49} and ovarian cancers^{50,51}.

Ca²⁺ is mainly stored in ER lumen, which is a critical regulator involved in cancer progression⁵². Accumulating evidences indicate that transient elevation of intracellular free Ca²⁺ can promote tumor cell migration and invasion. Conversely, sustained free Ca²⁺ stimulation might lead to the cell apoptosis and death⁵³. The disruption of Ca²⁺ homeostasis also triggers ERS, that is closely associated with EMT⁵⁴. For example, EMT is induced in breast cancer cells in parallel with the increase of cytosolic Ca²⁺, whereas chelating Ca²⁺ blocked the induction of EMT markers⁵⁵. CRT is considered as an intracellular Ca²⁺ regulator. It contains two Ca²⁺-binding domains: C-domain with a low affinity and high capacity region, and the P-domain with a high affinity and low capacity region⁵⁶. Thus, CRT deficiency generally leads to the decrease of intracellular Ca²⁺ storage^{57,58}. However, to our knowledge, there is no direct research involving the mechanism of CRT in regulating Ca²⁺-mediated EMT in PC. TG, as an effective inhibitor of SERCAs, causes an increase of cytoplasmic free Ca²⁺ concentration and further induces acute ERS via the depletion of Ca²⁺ from ER⁵⁹. We first found that CRT silencing inhibited TG-induced increase of intracellular free Ca²⁺ concentration. Meanwhile, TG-induced EMT in vitro by activating the key protein targets in EMT and ERK/MPK signaling (Slug, E-cad, ZO-1 and pERK), and enhancing cell mobility, which was also reversed by CRT silencing. Slug (also known as Snail2), is the most thoroughly investigated EMT regulator⁶⁰. As a transcription factor, Slug binds to the E-cadherin promoter to repress its transcription and triggers the steps of desmosomal disruption and cell spreading, which is the key step of the EMT process⁶¹. ERK signaling is also essential for EMT. An ERK-dependent epigenetic remodeling of regulatory elements results in a gene expression programme essential for driving EMT⁶². TGF-β1 activates ERK signaling, which is required for TGF-β1-mediated EMT in vitro⁶³. Musashi2 promotes EGF-induced EMT in PC via ZEB1-ERK/MAPK signaling⁶⁴. Taken together, CRT silencing inhibited TG-induced acute ERS and EMT via regulating Slug and ERK signaling in vitro. Interestingly, TG also induced IRE1α expression which was negatively regulated by CRT in vitro. IRE1α silencing enhanced TG-induced cell mobility. Thus, we next focused on the relationship between CRT and UPR in chronic ERS.

Chronic ERS produces endogenous or exogenous damage to cells and triggers an UPR response. IRE1α is the most evolutionally conserved one in UPR⁶⁵. As an ER type I transmembrane protein, the role of IRE1α in cancers is no longer simply considered as an oncogene or tumor suppressor, but a key component of cell fate switch, depending on different cancer types⁶⁶. IRE1α mediated apoptosis in human non-small cell lung cancer (NSCLC) A549 cells induced by a Tetramethylpyrazine analogue⁶⁷. However, IRE1α overexpression was associated with the resistant mechanism to osimertinib in NSCLC HCC827/OSIR Cells⁶⁸. Similarly, several studies have shown that IRE1α plays a contradictory role in colon cancer cells⁶⁹⁻⁷². We next found that CRT was co-immunoprecipitated and co-localized with IRE1α in vitro and its stable silencing caused chronic ERS by specifically activating IRE1α independent of IRE1/XBP1 axis. It is well known that IRE1/XBP1 axis plays a key role in mediating UPR in response to ERS⁷³. IRE1α/XBP1 pathway is a potential therapeutic target for Myc-driven cancers and multiple myeloma^{74,75}. However, IRE1 also exhibits XBP1-independent biochemical activities just shown in current study and previous reports^{76,77}. We next found that IRE1α silencing promoted EMT in vitro by enhancing cell mobility and activating EMT and ERK signaling, which was significantly reversed by CRT silencing. Interestingly, ERK1/2 activation is partially IRE1-dependent in mouse embryonic fibroblast cells treated with ER stress inducer⁷⁸, while IRE1 silencing attenuated ERK1/2 activation following ER stress in gastric cancer cells⁷⁹, which is inconsistent with current study. These inconsistent results might be due to the different cell types and microenvironment. Taken together, CRT silencing inhibited IRE1α silencing-induced chronic ERS and EMT via Slug and ERK signaling in PC cells, which has not been reported, to our knowledge.

Finally, CRT silencing inhibited subcutaneous tumor size and distant liver metastasis in vivo following with the increase of IRE1α expression. In human PC samples, CRT overexpression and IRE1α positive expression was positively and negatively associated with advanced clinical progression and poor survival of PC patients, respectively. Additionally, we found a

negative expression of CRT and IRE1 α in PC samples, which coordinately affected the patients' survival. These findings indicate that CRT and ERS pathways cooperatively contribute to the aggressive progression of PC.

Conclusion

In conclusion, for the first time, we demonstrated that CRT promoted EMT in PC via regulating TG-induced acute ERS and IRE1 α -mediated chronic ERS in intracellular free Ca²⁺ dependent manner via Slug and ERK signaling (Figure 9). However, we don't systematically investigate the dynamic exchange between intracellular free Ca²⁺ and ER Ca²⁺ in vitro, which might be the key step to explain above multi-process property. Future studies are needed to investigate the molecular mechanisms between CRT with Ca²⁺ homeostasis and ERS mediated EMT in PC.

List Of Abbreviations

PC: Pancreatic cancer; CRT: Calreticulin; ER: Endoplasmic reticulum; EMT: Epithelial-mesenchymal transition; ERS: Endoplasmic reticulum stress; UPR: Unfolded protein response; PERK: PKR-like endoplasmic reticulum kinase; IRE1 α : Inositol-requiring enzyme 1 α ; ATF-6: Activating transcription factor-6; PDAC: Pancreatic ductal adenocarcinoma; ATCC: American Type Culture Collection; FBS: Fetal bovine serum; TG: Thapsigargin; SERCAs: Sarcoplasmic/endoplasmic reticulum Ca²⁺-ATPases; HBSS: Hanks' Balanced Salt Solution; IHC: Immunohistochemistry; WB: Western blot; p-PERK: Phosphorylation PKR-like endoplasmic reticulum kinase; pERK: Phosphorylation extracellular regulated protein kinases; ERK: Extracellular regulated protein kinases; XBP1: X-box-binding protein 1; CoIP: Coimmunoprecipitation; HE: Hematoxylin and eosin; NSCLC: Non-small cell lung cancer

Declarations

Ethics approval and consent to participate

This study was approved by the academic committee at the First Hospital of China Medical University and written informed consent has been obtained from each patient.

Consent for publication

Not applicable.

Availability of data and material

Materials are available upon request.

Competing interests

The authors declare that they have no competing interest.

Funding

This work was supported by the Chinese National Science Foundation for youth scholar (No.81401941 to WS), the Chinese National Science Foundation (No. 81672835 to MD), the Scientific innovation plan from Young and middle-aged talents of Shenyang City [RC200357] and the Scientific research project of Education Department of Liaoning Province [L2020].

Authors' contributions

Conception and design: SW, WG, DM. Development of methodology: SW, WG, TJ, SX, CR, SJ, LY, JC, CC. Acquisition of data: WG, TJ, SJ, CC. Analysis and interpretation of data (statistical analysis, biostatistics, computational analysis): SJ, LY, JC. Writing, review and/or revision of manuscript: SW, WG, DM. Administrative, technical or material support: SX, CR, SJ. Study supervision: ZJ, DM. All authors read and approved the final manuscript.

Acknowledgements

We thank for the General Laboratory and the Center Laboratory of the First Hospital of China Medical University for technical supports.

Authors' information

¹Department of Gastrointestinal Surgery, The First Hospital, China Medical University, Shenyang, 110001, Liaoning, China.

²Department of General Surgery, The First Affiliated Hospital, Nanchang University, Nanchang, 330006, Jiangxi, China.

³Department of General Surgery, the People's Hospital of Liaoning province, Shenyang, 110034, Liaoning, China.

⁴Department of Clinical Laboratory, the Sixth Peoples' hospital of Shenyang, Shenyang, 110003, Liaoning, China

References

1. Siegel RL, Miller KD, Jemal A. Cancer Statistics, 2018. *CA Cancer J Clin.* 2018; 68:7-30.
2. Fucikova J, Kasikova L, Truxova I, Laco J, Skapa P, Ryska A et al. Relevance of the chaperone-like protein calreticulin for the biological behavior and clinical outcome of cancer. *Immunol Lett.* 2018; 193:25-34.
3. Sheng W, Chen C, Dong M, Zhou J, Liu Q, Dong Q et al. Overexpression of Calreticulin Contributes to the Development and Progression of Pancreatic Cancer. *J Cell Physiol.* 2014; 229(7):887-897.
4. Sheng W, Chen C, Dong M, Wang G, Zhou J, Song H et al. Calreticulin promotes EGF-induced EMT in pancreatic cancer cells via Integrin/EGFR-ERK/MAPK signaling pathway. *Cell Death Dis.* 2017; 8(10):e3147.
5. Limia CM, Sauzay C, Urrea H, Hetz C, Chevet E, Avril T. Emerging Roles of the Endoplasmic Reticulum Associated Unfolded Protein Response in Cancer Cell Migration and Invasion. *Cancers (Basel).* 2019;11(5).
6. Hsu SK, Chiu CC, Dahms HU, Chou CK, Cheng CM, Chang WT et al. Unfolded Protein Response (UPR) in Survival, Dormancy, Immunosuppression, Metastasis, and Treatments of Cancer Cells. *Int J Mol Sci.* 2019; 20(10):E2518.
7. Chen OI, Bobak YP, Stasyk OV, Kunz-Schughart LA. A Complex Scenario and Underestimated Challenge: The Tumor Microenvironment, ER Stress, and Cancer Treatment. *Curr Med Chem.* 2018; 25(21):2465-2502.
8. Kültz D. Molecular and evolutionary basis of the cellular stress response. *Annu Rev Physiol.* 2005; 67:225-57.
9. Fulda S, Gorman AM, Hori O, Samali A. Cellular stress responses: cell survival and cell death. *Int J Cell Biol.* 2010; 2010:214074.

10. Singh J, Hussain Y, Luqman S, Meena A. TargetingCa²⁺ signalling through phytomolecules to combat cancer. *Pharmacol Res.* 2019; 146:104282.
11. Bernales S, Soto MM, McCullagh E. Unfolded protein stress in the endoplasmic reticulum and mitochondria: a role in neurodegeneration. *Front Aging Neurosci.* 2012; 4:5.
12. Santoni G, Morelli MB, Marinelli O, Nabissi M, Santoni M, Amantini C. Calcium Signaling and the Regulation of Chemosensitivity in Cancer Cells: Role of the Transient Receptor Potential Channels. *Adv Exp Med Biol.* 2020; 1131:505-517.
13. Dibdiakova K, Saksonova S, Pilchova I, Klacanova K, Tatarkova Z, Racay P. Both thapsigargin- and tunicamycin induced endoplasmic reticulum stress increases expression of Hrd1 in IRE1-dependent fashion. *Neurol Res.*2019; 41(2):177-188.
14. Wang G, Sheng W, Shi X, Li X, Zhou J, Dong M. Serine/arginine protein-specific kinase 2 promotes the development and progression of pancreatic cancer by downregulating Numb and p53. *FEBS J.*2019; 286(9):1668-1682.
15. Liu L, Wu N, Wang Y, Zhang X, Xia B, Tang J et al. TRPM7 promotes the epithelial-mesenchymal transition in ovarian cancer through the calcium-related PI3K / AKT oncogenic signaling. *J Exp Clin Cancer Res.* 2019; 38(1):106.
16. Moon SY, Kim HS, Nho KW, Jang YJ, Lee SK. Endoplasmic reticulum stress induces epithelial-mesenchymal transition through autophagy via activation of c-Src kinase. *Nephron Exp Nephrol.* 2014; 126(3):127-140.
17. Shin HS, Ryu ES, Oh ES, Kang DH. Endoplasmic reticulum stress as a novel target to ameliorate epithelial-to-mesenchymal transition and apoptosis of human peritoneal mesothelial cells. *Lab Invest.* 2015; 95(10):1157-1173.
18. Wu L, Huang X, Kuang Y, Xing Z, Deng X, Luo Z.
Thapsigargin induces apoptosis in adrenocortical carcinoma by activatingendoplasmic reticulum stress and the JNK signaling pathway: an in vitro and in vivo study. *Drug Des Devel Ther.*2019; 13:2787-2798.
19. Lin Y, Jiang M, Chen W, Zhao T, Wei Y. Cancer and ER stress: Mutual crosstalk between autophagy, oxidative stress and inflammatory response. *Biomed Pharmacother.*2019; 118:109249.
20. Ruiz A, Matute C, Alberdi E. Intracellular Ca²⁺ release through ryanodine receptors contributes to AMPA receptor-mediated mitochondrial dysfunction and ER stress in oligodendrocytes. *Cell Death Dis.*2010; 1:e54.
21. Butler MR, Ma H, Yang F, Belcher J, Le YZ, Mikoshiba K et al. Endoplasmic reticulum (ER) Ca²⁺-channel activity contributes to ER stress and cone death in cyclic nucleotide-gated channel deficiency. *J Biol Chem.*2017; 292(27):11189-11205.
22. Sheng X, Nenseth HZ, Qu S, Kuzu OF, Frahnnow T, Simon L et al. IRE1 α -XBP1s pathway promotes prostate cancer by activating c-MYC signaling. *Nat Commun.* 2019; 10(1):323.
23. Auf G, Jabouille A, Guérit S, Pineau R, Delugin M, Bouche-careilh M et al. Inositol-requiring enzyme 1 α is a key regulator of angiogenesis and invasion in malignant glioma. *Proc Natl Acad Sci U S A.* 2010; 107(35):15553-15558.
24. Li H, Chen X, Gao Y, Wu J, Zeng F, Song F. XBP1 induces snail expression to promote epithelial- to-mesenchymal transition and invasion of breast cancer cells. *Cell Signal.*2015; 27(1):82-89.
25. Bray F, Ferlay J, Soerjomataram I, Siegel RL, Torre LA, Jemal A. Global Cancer Statistics 2018: GLOBOCAN Estimates of Incidence and Mortality Worldwide for 36 Cancers in 185 Countries. *CA Cancer J Clin.* 2018; 68(6):394-424.
26. Wang S, Huang S, Sun YL. Epithelial-Mesenchymal Transition inPancreatic Cancer: A Review. *Biomed Res Int.* 2017; 2017:2646148.
27. Guarino M, Rubino B, Ballabio G. The role of epithelial-mesenchymal transition in cancer pathology. *Pathology.* 2007; 39(3):305–318.
28. Guarino M. Guarino M. Epithelial-mesenchymal transition and tumour invasion. *Int J Biochem Cell Biol.* 2007; 39(12):2153–2160.
29. Ostwald TJ, MacLennan DH. Isolation of a high affinity calcium binding protein from sarcoplasmic reticulum. *J Biol Chem.*1974; 249(3):974-979.

30. Lu YC, Weng WC, Lee H. Functional roles of calreticulin in cancer biology. *Biomed Res Int.* 2015; 2015:526524.
31. Venkateswaran K, Verma A, Bhatt AN, Shrivastava A, Manda K, Raj HG et al. Emerging Roles of Calreticulin in Cancer: Implications for Therapy. *Curr Protein Pept Sci.*2018; 19(4):344-357.
32. Mohammadreza Zamanian, Abhi Veerakumarasivam, Syahril Abdullah, Rozita Rosli. Calreticulin and Cancer. *Pathol Oncol Res.* 2013; 19:149–154
33. Liu R, Gong J, Chen J, Li Q, Song C, Zhang J et al. Calreticulin as a potential diagnostic biomarker for lung cancer. *Cancer Immunol Immunother.* 2012; 61(6):855-864.
34. Zamanian M, Qader Hamadneh LA, Veerakumarasivam A, Abdul Rahman S, Shohaimi S, Rosli R. Calreticulin mediates an invasive breast cancer phenotype through the transcriptional dysregulation of p53 and MAPK pathways. *CancerCell Int.* 2016; 16:56.
35. Lwin ZM, Guo C, Salim A, Yip GW, Chew FT, Nan J et al. Clinicopathological significance of calreticulin in breast invasive ductal carcinoma. *Mod Pathol.*2010; 23(12):1559-1566.
36. Chen CN, Chang CC, Su TE, Hsu WM, Jeng YM, Ho MC et al. Identification of Calreticulin as a Prognosis Marker and Angiogenic Regulator in Human Gastric Cancer. *Ann Surg Oncol.*2009; 16(2):524-33.
37. Yoon GS, Lee H, Jung Y, Yu E, Moon HB, Song K et al. Nuclear matrix of calreticulin in hepatocellular carcinoma. *Cancer Res.*2000; 60(4):1117-1120.
38. Lu YC, Chen CN, Wang B, Hsu WM, Chen ST, Chang KJ et al. Changes in tumor growth and metastatic capacities of J82 human bladder cancer cells suppressed by down-regulation of calreticulin expression. *Am J Pathol.*2011; 179(3):1425-1433
39. Chiang WF, Hwang TZ, Hour TC, Wang LH, Chiu CC, Chen HR et al. Calreticulin, an endoplasmic reticulum-resident protein, is highly expressed and essential for cell proliferation and migration in oral squamous cell carcinoma. *Oral Oncol.* 2013; 49(6):534-541.
40. Du XL, Yang H, Liu SG, Luo ML, Hao JJ, Zhang Y et al. Calreticulin promotes cell motility and enhances resistance to anoikis through STAT3-CTTN-Akt pathway in esophageal squamous cell carcinoma. 2009; 28(42):3714-3722.
41. Shi F, Shang L, Pan BQ, Wang XM, Jiang YY, Hao JJ et al. Calreticulin promotes migration and invasion of esophageal cancer cells by up-regulating neuropilin-1 expression via STAT5A. *Clin Cancer Res.* 2014; 20(23):6153-6162.
42. Hsu WM, Hsieh FJ, Jeng YM, Kuo ML, Chen CN, Lai DM et al. Calreticulin expression in neuroblastoma-a novel independent prognostic factor. *Ann Oncol.* 2005; 16(2):314-321.
43. Shih YY, Nakagawara A, Lee H, Juan HF, Jeng YM, Lin DT et al. Calreticulin Mediates Nerve Growth Factor-Induced Neuronal Differentiation. *J Mol Neurosci.* 2012; 47(3):571-581.
44. Toquet C, Jarry A, Bou-Hanna C, Bach K, Denis MG, Mosnier JF et al. Altered Calreticulin expression in human colon cancer: maintenance of Calreticulin expression is associated with mucinous differentiation. *Oncol Rep.*2007; 17(5):1101-1107.
45. Peng RQ, Chen YB, Ding Y, Zhang R, Zhang X, Yu XJ et al. Expression of calreticulin is associated with infiltration of T-cells in stage B colon cancer. *World J Gastroenterol.*2010; 16(19):2428-2434.
46. Vougas K, Gaitanarou E, Marinou E, Kittas C, Voloudakis-Baltatzis IE.. Two-dimensional electrophoresis and immunohistochemical study of calreticulin in colorectal adenocarcinoma and mirror biopsies. *J BUON.*2008; 13(1):101-107.
47. Alfonso P, Núñez A, Madoz-Gurpide J, Lombardía L, Sánchez L, Casal JI. Proteomic expression analysis of colorectal cancer by two-dimensional differential gel electrophoresis. *Proteomics.* 2005; 5(10):2602-2611.
48. Alur M, Nguyen MM, Eggner SE, Jiang F, Dadras SS, Stern J et al. Suppressing roles of calreticulin in prostate cancer growth and metastasis. *Am J Pathol.*2009; 175(2):882-890.
49. Alaiya A, Roblick U, Egevad L, Carlsson A, Franzén B, Volz D et al. Polypeptide expression in prostate hyperplasia and prostate adenocarcinoma. *Anal Cell Pathol.* 2000; 21(1):1-9.

50. Vaksman O, Davidson B, Tropé C, Reich R. Calreticulin expression is reduced in high-grade ovarian serous carcinoma effusions compared with primary tumors and solid metastases. *Hum Pathol.*2013; 44(12):2677-2683.
51. Hellman K, Alaiya AA, Schedvins K, Steinberg W, Hellström AC, Auer G. Protein expression patterns in primary carcinoma of the vagina. *Br J Cancer.*2004; 91(2):319-326.
52. White C. The regulation of tumor cell invasion and metastasis by endoplasmic reticulum-to-mitochondrial Ca²⁺ transfer. *Front Oncol.*2017; 7:171.
53. Bong AHL, Monteith GR. Calcium signaling and the therapeutic targeting of cancer cells. *Biochim Biophys Acta Mol Cell Res.* 2018; 1865:1786-1794.
54. Iamshanova O, Fiorio Pla A, Prevarskaya N, Molecular mechanisms of tumor invasion: regulation by calcium signals. *J Physiol.* 2017; 595(10):3063-3075.
55. Davis FM, Azimi I, Faville RA, Peters AA, Jalink K, Putney JW Jr et al. Induction of epithelial–mesenchymal transition (EMT) in breast cancer cells is calcium signal dependent. *Oncogene.* 2014; 33(18):2307-2316.
56. Michalak M, Corbett EF, Mesaeli N, Nakamura K, Opas M. Calreticulin: one protein, one gene, many functions. *Biochem J.* 1999; 344:281-292.
57. Bastianutto C, Clementi E, Codazzi F, Podini P, De Giorgi F, Rizzuto R et al. Overexpression of calreticulin increases the Ca²⁺ capacity of rapidly exchanging Ca²⁺ stores and reveals aspects of their luminal microenvironment and function. *J Cell Biol.*1995; 130(4):847-855.
58. Mery L, Mesaeli N, Michalak M, Opas M, Lew DP, Krause KH. Overexpression of calreticulin increases intracellular Ca²⁺ storage and decreases store-operated Ca²⁺ influx. *J Biol Chem.* 1996; 271(16):9332-9339.
59. Thastrup O, Cullen PJ, Drøbak BK, Hanley MR, Dawson AP. Thapsigargin, a tumor promoter, discharges intracellular Ca²⁺ stores by specific inhibition of the endoplasmic reticulum Ca²⁺(+)-ATPase. *Proc Natl Acad Sci U S A.* 1990; 87(7):2466-2470.
60. Hotz B, Arndt M, Dullat S, Bhargava S, Buhr HJ, Hotz HG. Epithelial to mesenchymal transition: expression of the regulators snail, slug, and twist in pancreatic cancer. *Clin Cancer Res.* 2007; 13(16):4769-4776.
61. Ganiou Assani, Yunfeng Zhou. Effect of Modulation of Epithelial-Mesenchymal Transition Regulators Snail1 and Snail2 on Cancer Cell Radiosensitivity by Targeting of the Cell Cycle, Cell Apoptosis and Cell Migration/Invasion. *Oncol Lett,* 2019; 17(1):23-30.
62. Mohit Navandar, Angela Garding, Sanjeeb Kumar Sahu, Abhijeet Pataskar, Sandra Schick, Vijay K Tiwari. ERK Signalling Modulates Epigenome to Drive Epithelial to Mesenchymal Transition. *Oncotarget,* 2017; 8(17):29269-29281.
63. Lu Xie, Brian K Law, Anna M Chytil, Kimberly A Brown, Mary E Aakre, Harold L Moses. Activation of the Erk Pathway Is Required for TGF-beta1-induced EMT in Vitro. *Neoplasia,* 2004; 6(5):603-10.
64. Weiwei Sheng, Xiaoyang Shi, Yiheng Lin, Jingtong Tang, Chao Jia, Rongxian Cao et al. Musashi2 Promotes EGF-induced EMT in Pancreatic Cancer via ZEB1-ERK/MAPK Signaling. *J Exp Clin Cancer Res,* 2020; 39(1):16.
65. Chalmers F, Mogre S, Son J, Blazanin N, Glick AB. The multiplex roles of the unfolded protein response regulator IRE1α in cancer. *Mol Carcinog.* 2019; 58(9):1623-1630.
66. Wu Y, Shan B, Dai J, Xia Z, Cai J, Chen T et al. Dual role for inositol-requiring enzyme 1α in promoting the development of hepatocellular carcinoma during diet-induced obesity in mice. 2018; 68(2):533-546.
67. Zhang J, Liang Y, Lin Y, Liu Y, You Y, Yin W. IRE1α-TRAF2-ASK1 pathway is involved in CSTMP-induced apoptosis and ER stress in human non-small cell lung cancer A549 cells. *Biomed Pharmacother.*2016; 82:281-289.
68. Tang ZH, Su MX, Guo X, Jiang XM, Jia L, Chen X et al. Increased expression of IRE1α Associates with the Resistant Mechanism of Osimertinib (AZD9291)-resistant non-small Cell Lung Cancer HCC827/OSIR Cells. *Anticancer Agents Med Chem.* 2018; 18(4):550-555.
69. Li XX, Zhang HS, Xu YM, Zhang RJ, Chen Y, Fan L et al. Knockdown of IRE1 inhibits colonic tumorigenesis through decreasing β-catenin and IRE1α targeting suppresses colon cancer cells. 2017; 36(48):6738-6746.

70. Xie Y, Liu C, Qin Y, Chen J, Fang J. Knockdown of IRE1 α suppresses metastatic potential of colon cancer cells through inhibiting FN1-Src/FAK-GTPases signaling. *Int J Biochem Cell Biol*. 2019; 114:105572.
71. Banerjee A, Ahmed H, Yang P, Czinn SJ, Blanchard TG. Endoplasmic reticulum stress and IRE-1 signaling cause apoptosis in colon cancer cells in response to andrographolide treatment. 2016; 7(27):41432-41444.
72. Chern YJ, Wong JCT, Cheng GSW, Yu A, Yin Y, Schaeffer DF et al. The interaction between SPARC and GRP78 interferes with ER stress signaling and potentiates apoptosis via PERK/eIF2 α and IRE1 α /XBP-1 in colorectal cancer. *Cell Death Dis*. 2019; 10(7):504.
73. Rong Wu, Qing-Hai Zhang, Yan-Ju Lu, Kun Ren, Guang-Hui Yi. Involvement of the IRE1 α -XBP1 Pathway and XBP1s-dependent Transcriptional Reprogramming in Metabolic Diseases. *DNA Cell Biol*, 2015; 34(1):6-18.
74. Hong Xie, Chih-Hang Anthony Tang, Jun H Song, Anthony Mancuso, Juan R Del Valle, Jin Cao et al. IRE1 α RNase-dependent Lipid Homeostasis Promotes Survival in Myc-transformed Cancers. *J Clin Invest*, 2018; 128(4):1300-1316.
75. Lin Chen, Qian Li, Tiantian She, Han Li, Yuanfang Yue, Shuang Gao et al. IRE1 α -XBP1 Signaling Pathway, a Potential Therapeutic Target in Multiple Myeloma. *Leuk Res*, 2016; 49:7-12.
76. Huai-Wei Huang, Xiaomei Zeng, Taiyoun Rhim, David Ron, Hyung Don Ryoo. The Requirement of IRE1 and XBP1 in Resolving Physiological Stress During Drosophila Development. *J Cell Sci*, 2017; 130(18):3040-3049.
77. Tokiro Ishikawa, Makoto Kashima, Atsushi J Nagano, Tomoko Ishikawa-Fujiwara, Yasuhiro Kamei, Takeshi Todo et al. Unfolded Protein Response Transducer IRE1-mediated Signaling Independent of XBP1 mRNA Splicing Is Not Required for Growth and Development of Medaka Fish. *Elife*, 2017; 6:e26845.
78. Duc Thang Nguyễn, Sem Kebache, Ali Fazel, Hetty N Wong, Sarah Jenna, Anouk Emadali et al. Nck-dependent Activation of Extracellular Signal-Regulated kinase-1 and Regulation of Cell Survival During Endoplasmic Reticulum Stress. *Mol Biol Cell*, 2004; 15(9):4248-60.
79. Lin Jie Zhang, Si Chen, Pin Wu, Chun Song Hu, Rick F Thorne, Chang Ming Luo et al. Inhibition of MEK Blocks GRP78 Up-Regulation and Enhances Apoptosis Induced by ER Stress in Gastric Cancer Cells. *Cancer Lett*, 2009; 274(1):40-6.

Tables

Table 1
Association of CRT and IRE1 α expression with clinicopathological data in PC patients.

Parameters	No. of patients	CRT		P	IRE1 α		P
		Low	High		Negative	Positive	
Cases	81	31	50		43	38	
Age (years)							
≤ 65	63	25	38	0.625	36	27	0.171
> 65	18	6	12		7	11	
Gender							
Male	47	19	28	0.639	21	26	0.075
Female	34	12	22		22	12	
Tumor location							
Head	57	21	36	0.683	30	27	0.899
Body-tail	24	10	14		13	11	
Tumor size (cm)							
< 3	24	7	17	0.274	13	11	0.899
≥ 3	57	24	33		30	27	
Differentiation							
Well	22	7	15	0.466	12	10	0.872
Moderate and poor	59	24	35		31	28	
T stage							
T1 + T2	72	30	42	0.157	37	35	0.609
T3 + T4	9	1	8		6	3	
Lymph nodes metastasis							
N0 (negative)	65	30	35	0.003	30	35	0.012
N1 (positive)	16	1	15		13	3	
UICC stage							
I + IIA	62	29	33	0.004	27	35	0.002
IIB + III	19	2	17		16	3	
Perineural invasion							
Absent	70	28	42	0.636	37	33	0.917
Present	11	3	8		6	5	
Vascular permeation							
Absent	49	15	34	0.079	28	21	0.365
Present	32	16	16		15	17	

Parameters	No. of patients	CRT		P	IRE1α		P
Pre-therapeutic CA19-9 level (U/ml)							
< 37	22	12	10	0.066	8	14	0.066
≥ 37	59	19	40		35	24	
Postoperative liver metastasis							
Negative	54	23	31	0.258	27	27	0.431
Positive	27	8	19		16	11	

Table 2
Correlation analysis of the relationship between CRT with IRE1α.

Parameter	CRT		r rank	P
	Low (n = 31)	High (n = 50)		
IRE1α			-0.278	0.012
Negative (n = 43)	11	32		
Positive (n = 38)	20	18		

Figures

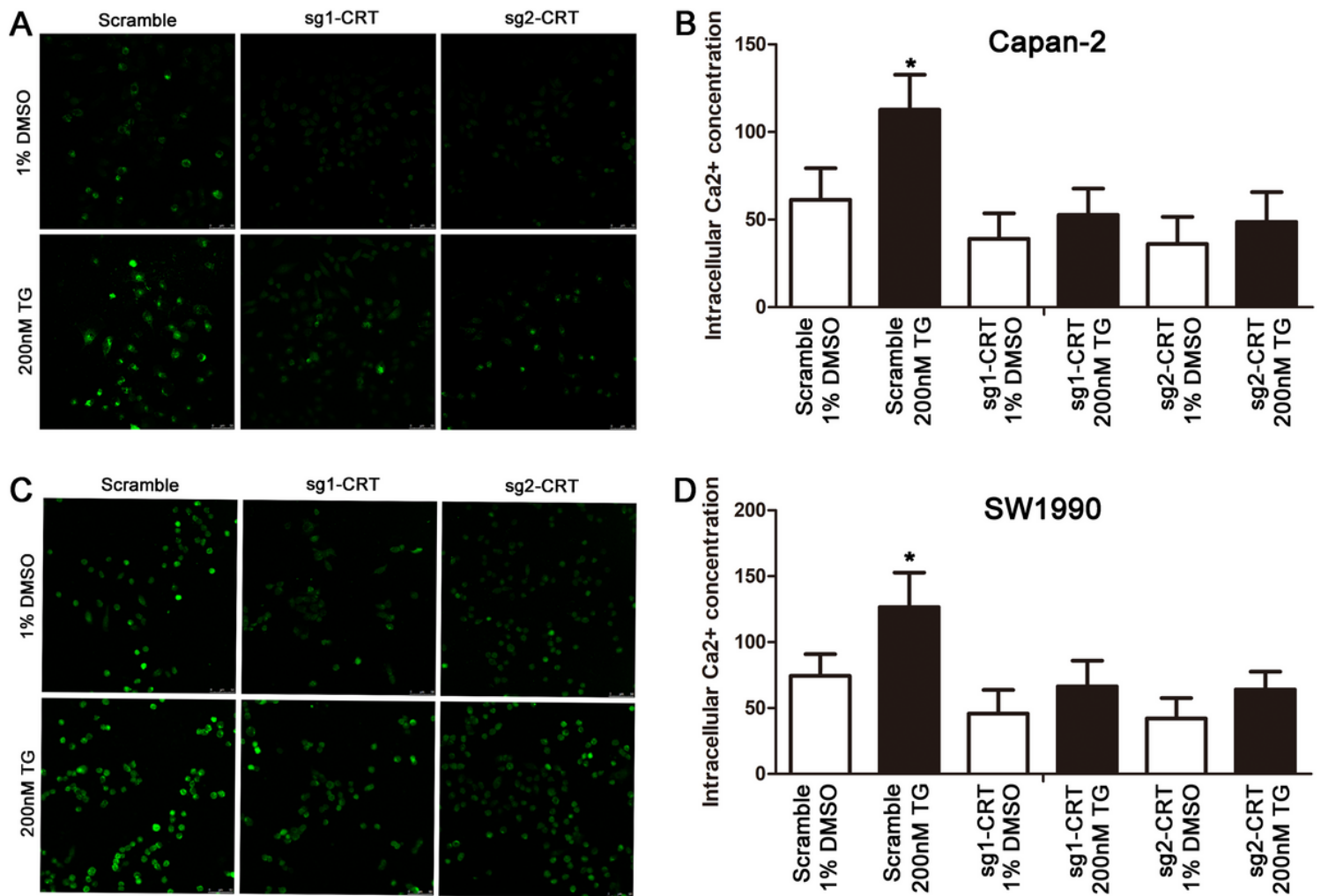


Figure 1

CRT silencing inhibited TG-induced the increase of intracellular free Ca²⁺ concentration in vitro. A, B The intracellular free Ca²⁺ concentration in Capan-2 cells detected by confocal microscopy (A) or flow cytometry (B), respectively. C, D The intracellular free Ca²⁺ concentration in SW1990 cells detected by confocal microscopy (C) or flow cytometry (D), respectively. TG: Thapsigargin. Data are shown as mean \pm SD. *P < 0.05 versus control.

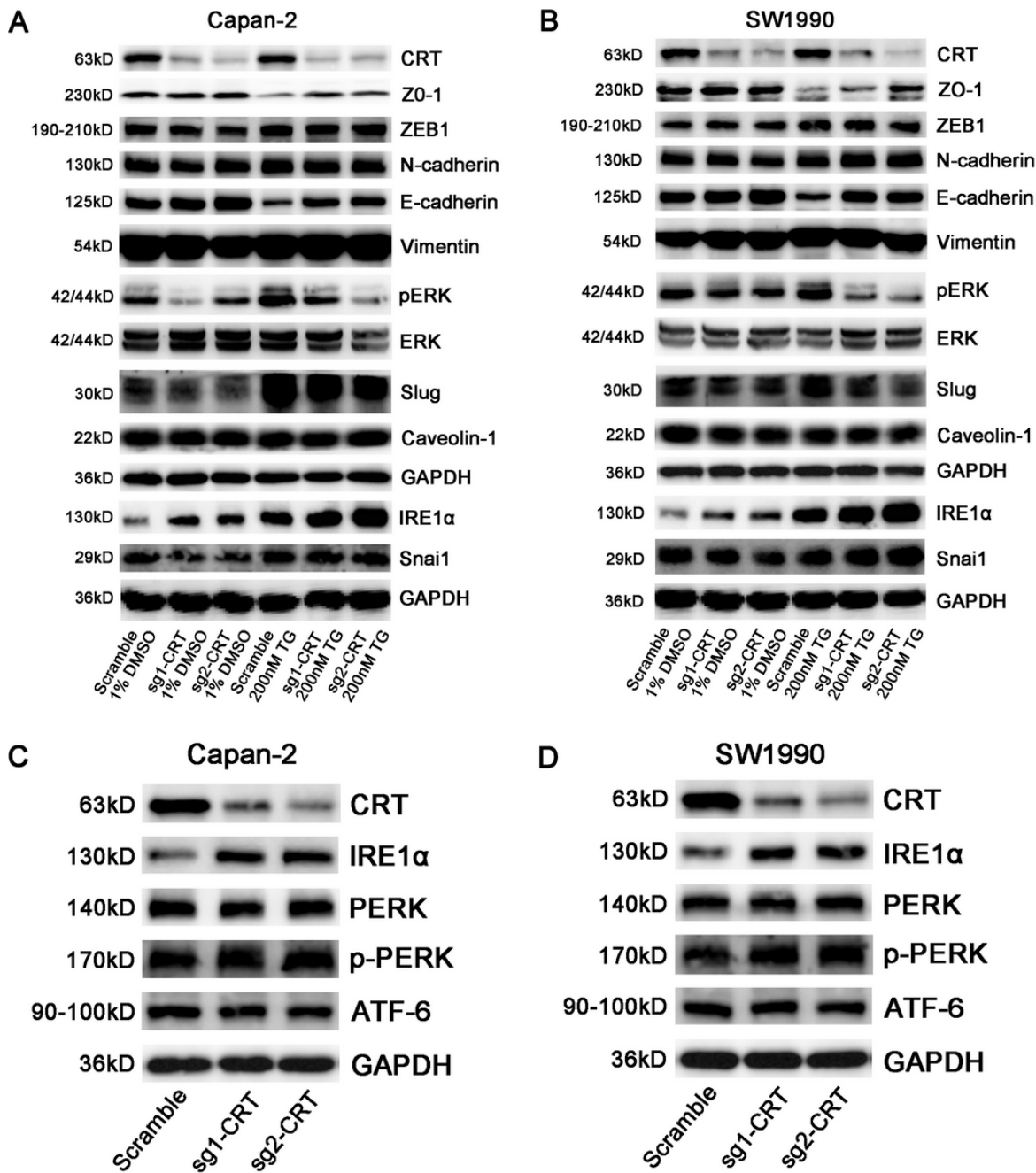


Figure 2

The effect of CRT silencing in TG-induced EMT and UPR activation in vitro by WB. A The expression of EMT classic markers in scramble, sg1-CRT and sg2-CRT transfected Capan-2 cells with or without TG treatment. B The expression of EMT classic markers in scramble, sg1-CRT and sg2-CRT transfected SW1990 cells with or without TG treatment. C, D The expression of UPR family: IRE1α, PERK and ATF-6 in CRT silencing Capan-2 (C) and SW1990 (D) cells. TG: Thapsigargin. The statistic data of WB was shown in Supplemental Figure 2.

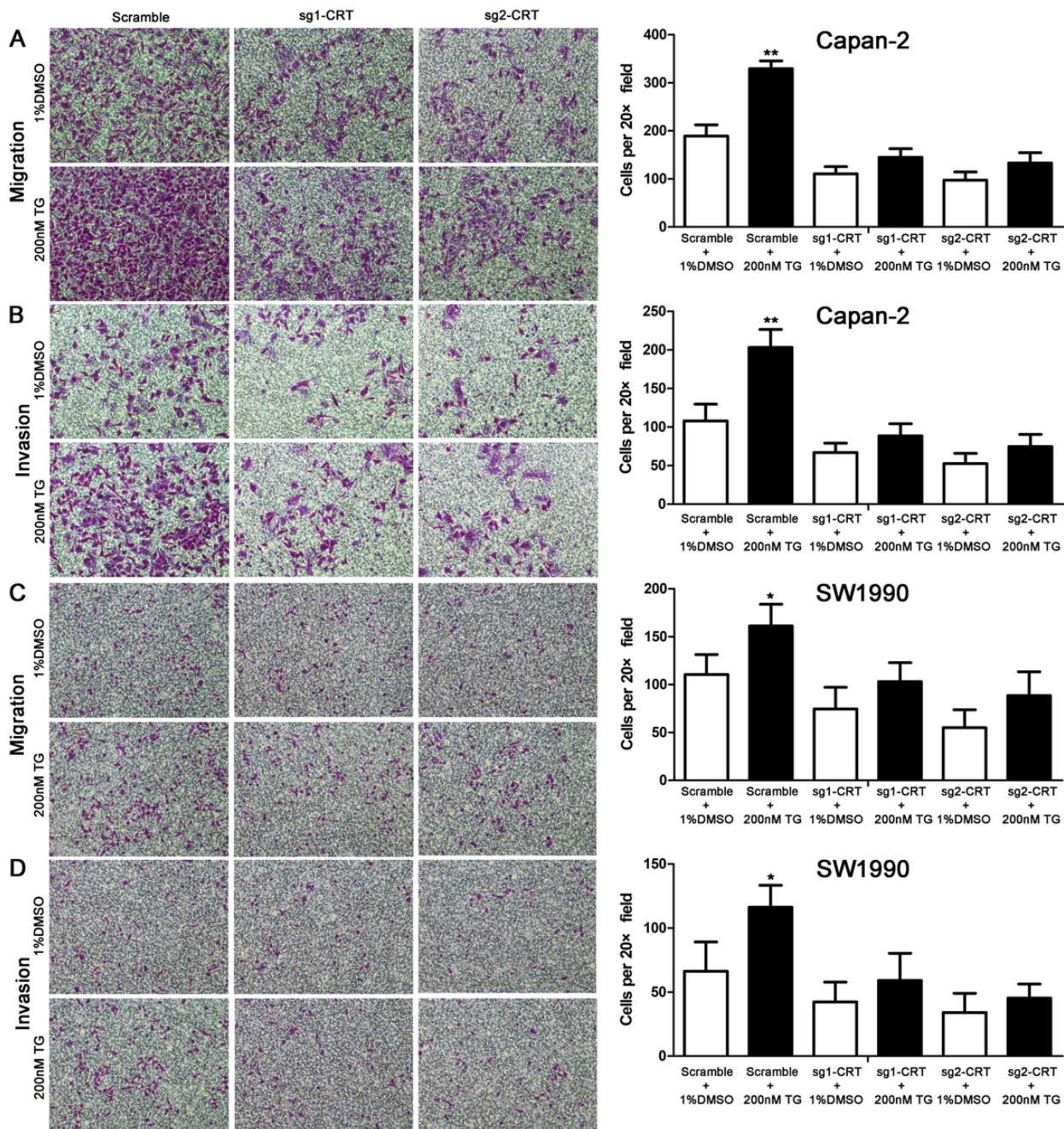


Figure 3

CRT silencing inhibited TG-induced the increase of cell migration and invasion in vitro. A, B CRT silencing inhibited TG-induced the increase of cell migration (A) and invasion (B) in Capan-2 cells. C, D CRT silencing inhibited TG-induced the increase of cell migration (C) and invasion (D) in SW1990 cells. TG: Thapsigargin. Data are shown as mean \pm SD. *P < 0.05, **P < 0.01 versus control.

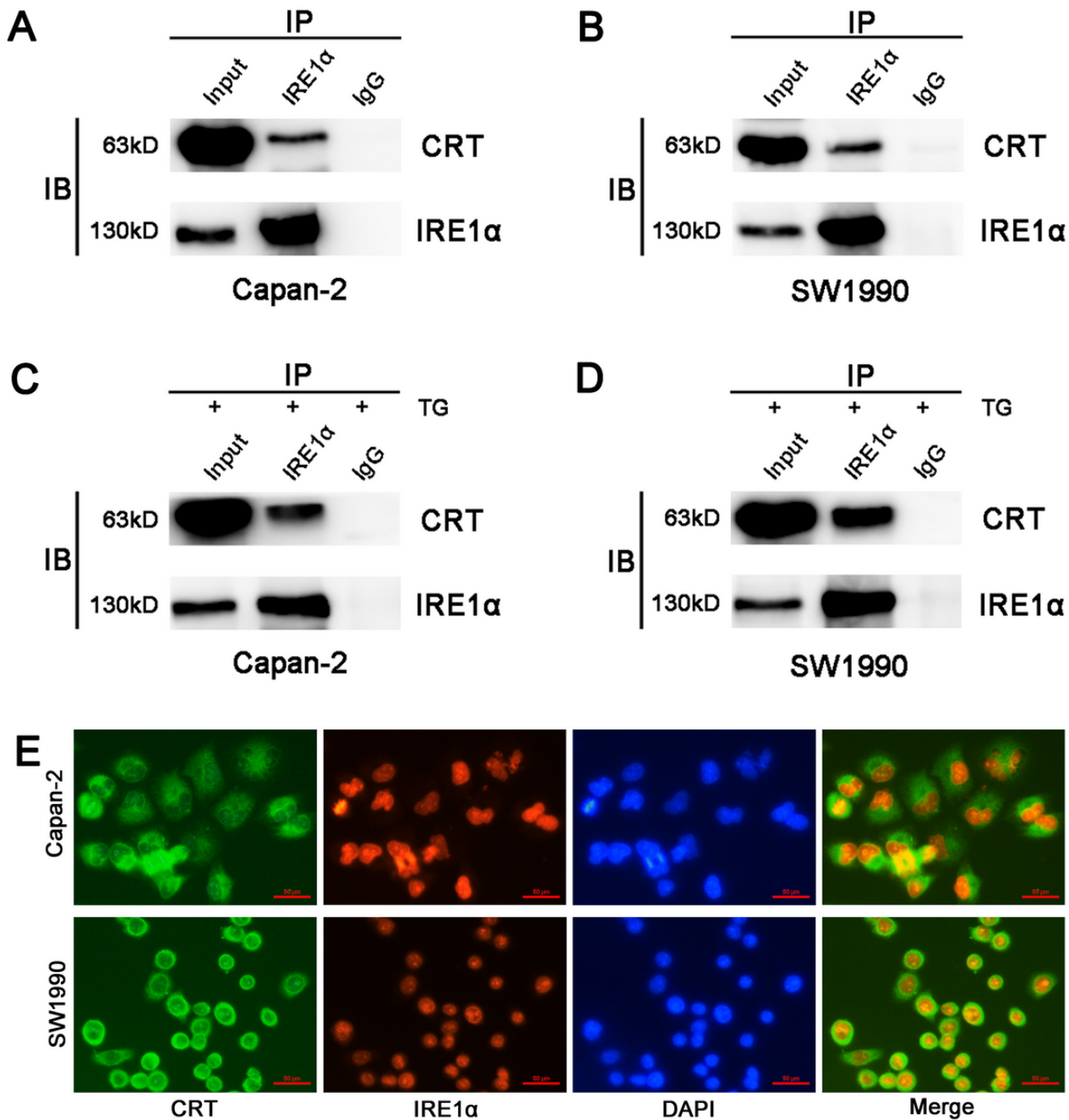


Figure 4

The close interaction between CRT and IRE1α in vitro detected by IP and IF. A, C CRT was coimmunoprecipitated with IRE1α in the lysates of Capan-2 cells without (A) or with (C) TG treatment. B, D CRT was coimmunoprecipitated with IRE1α in the lysates of SW1990 cells without (B) or with (D) TG treatment. E CRT was partially co-localized with IRE1α in Capan-2 and SW1990 cells. TG: Thapsigargin. CRT stained with FITC. IRE1α stained with TRIC.

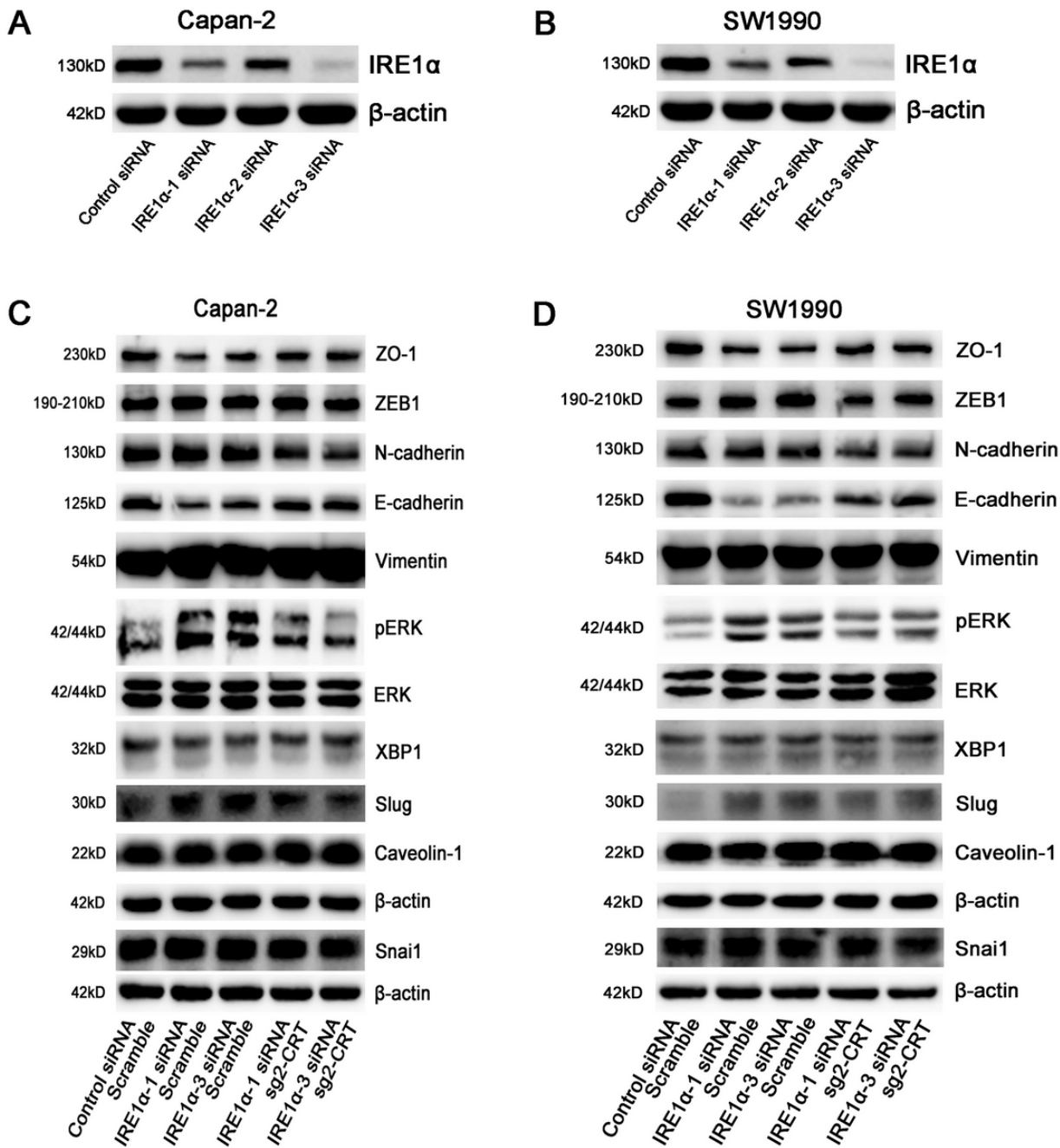


Figure 5

CRT silencing inhibited IRE1α silencing-induced the changes of EMT markers in vitro. A, B The expression of IRE1α in control siRNA, IRE1α-1 siRNA, IRE1α-2 siRNA and IRE1α-3 siRNA transfected Capan-2 (A) and SW1990 (B) cells. C, D The expression of EMT classic markers in Capan-2 (C) and SW1990 (D) cells transfected with the combinations shown. The statistic data of WB was shown in Supplemental Figure 3.

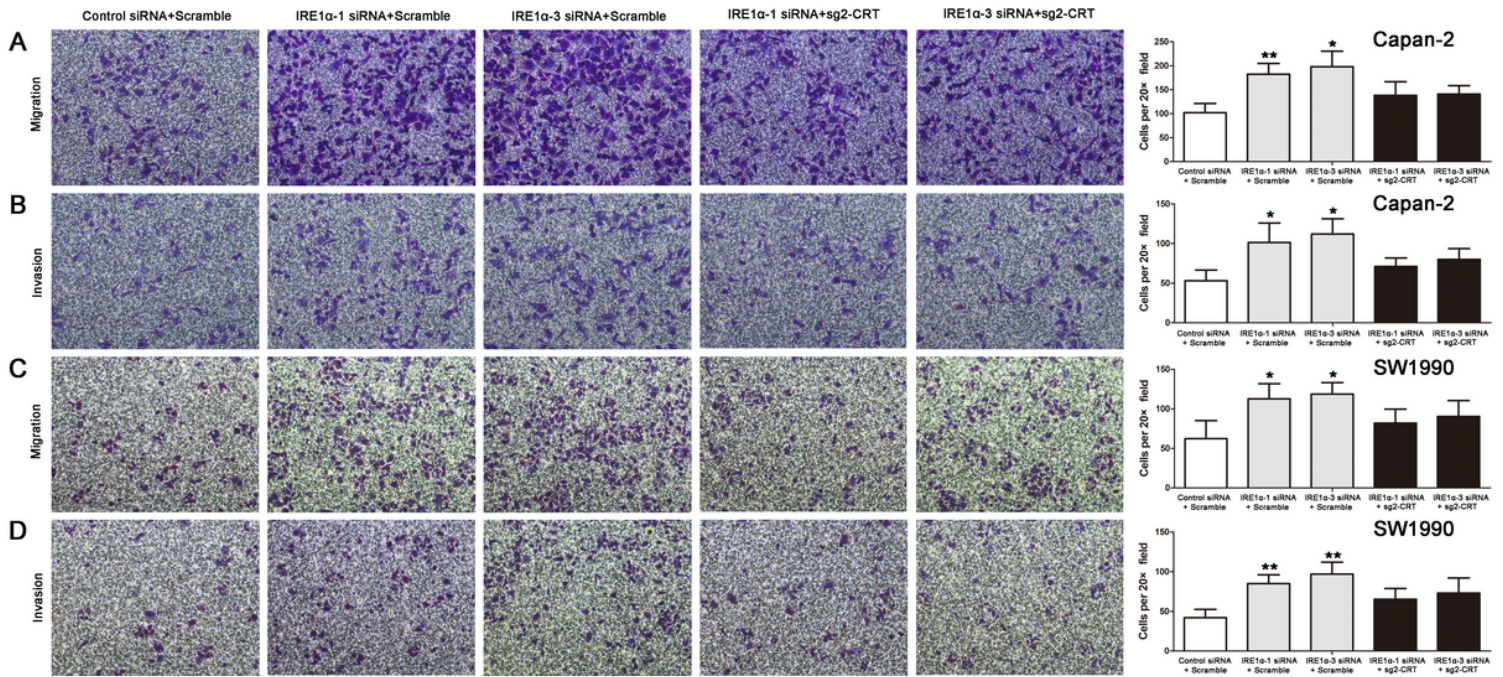


Figure 6

CRT silencing inhibited IRE1 α silencing-induced the increase of cell migration and invasion in vitro. A, B Cell migration (A) and invasion (B) in Capan-2 cells transfected with the combinations shown. C, D Cell migration (C) and invasion (D) in SW1990 cells transfected with the combinations shown. Data are shown as mean \pm SD. *P < 0.05, **P < 0.01 versus control.

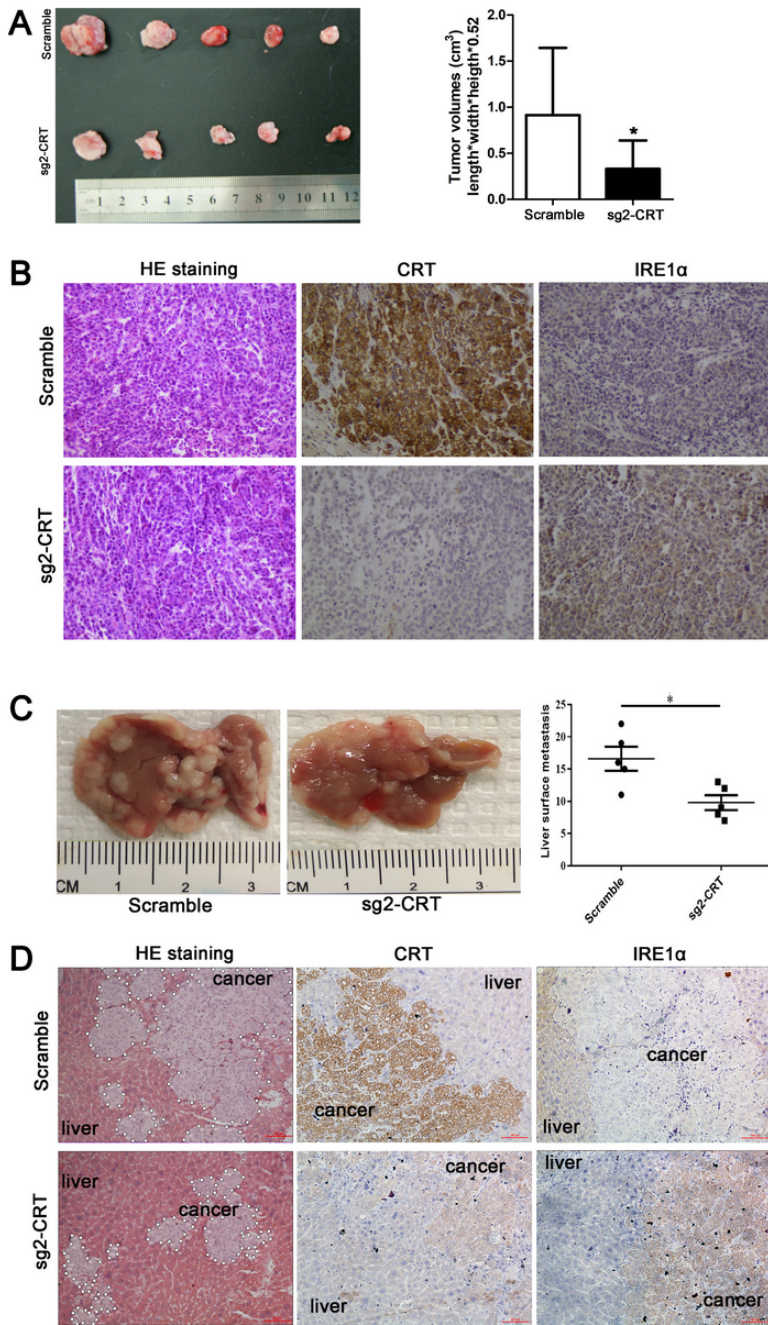


Figure 7

CRT silencing inhibited subcutaneous tumor size and distant liver metastasis in vivo. A The representative images and statistical data of tumor volumes between scramble and sg2-CRT groups in nude mice. B The representative HE and IHC images of CRT and IRE1α expression in subcutaneous tumor between scramble and sg2-CRT groups. C The representative images and statistical data of the number of liver metastases between scramble and sg2-CRT groups in nude mice. D The representative HE and IHC images of CRT and IRE1α expression in distant liver metastasis between scramble and sg2-CRT groups. Data are shown as mean ± SD. *P < 0.05 versus control. Data are shown as mean ± SD. *P < 0.05 versus control.

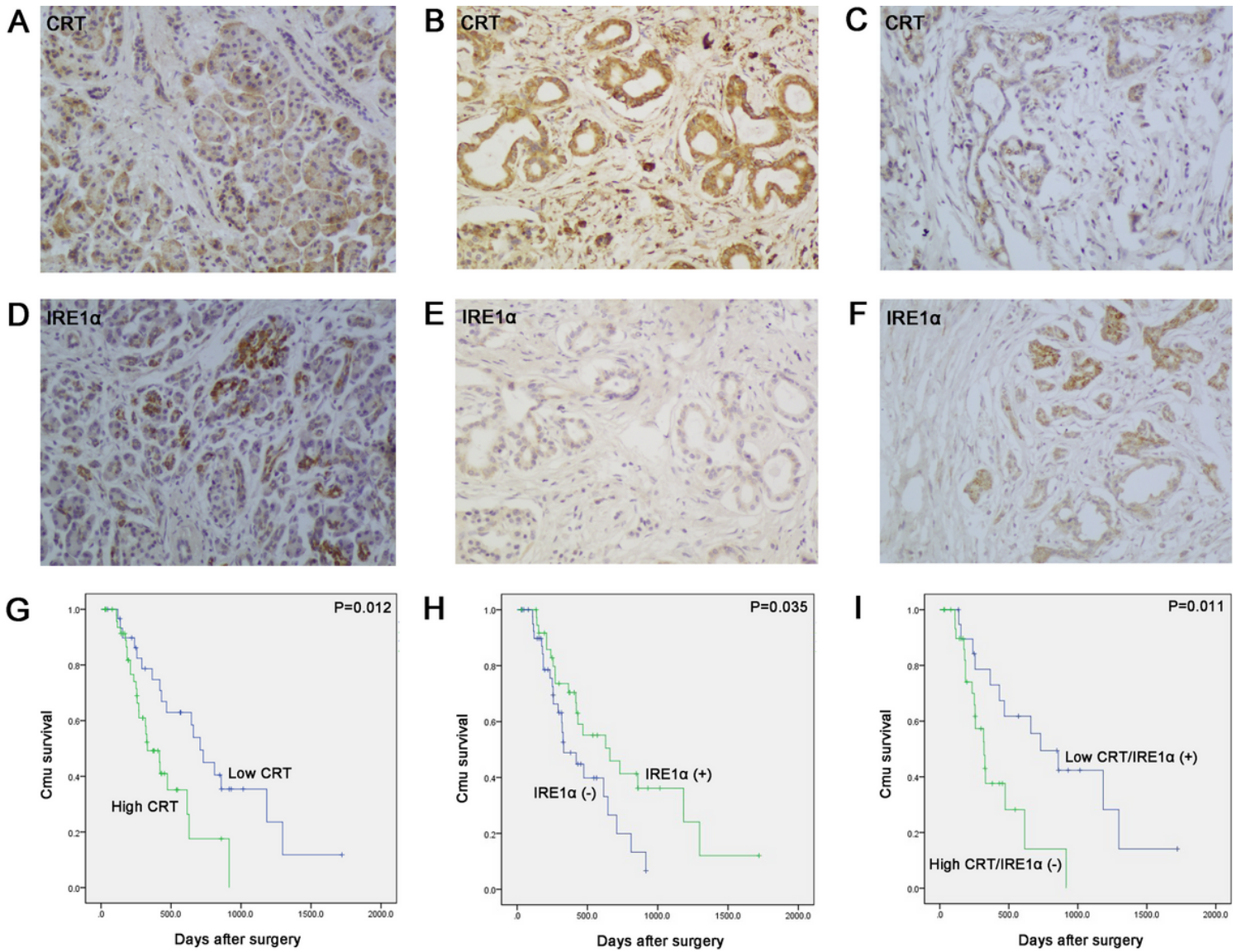


Figure 8

The negative relationship of CRT and IRE1α expression in human PC samples was coordinately associated with the survival of PC patients. A, D Low CRT (A) and positive IRE1α (D) expression in normal pancreas. B, E High CRT (B) and negative IRE1α (E) expression in one serial PC sample. C, F Low CRT (C) and positive IRE1α (F) expression in another serial PC sample. G Kaplan–Meier curves for patients with high versus low CRT expression in tumors. H Kaplan–Meier curves for patients with positive (+) versus negative (-) IRE1α expression in tumors. I Kaplan–Meier curves for patients with the co-expression of CRT and IRE1α.

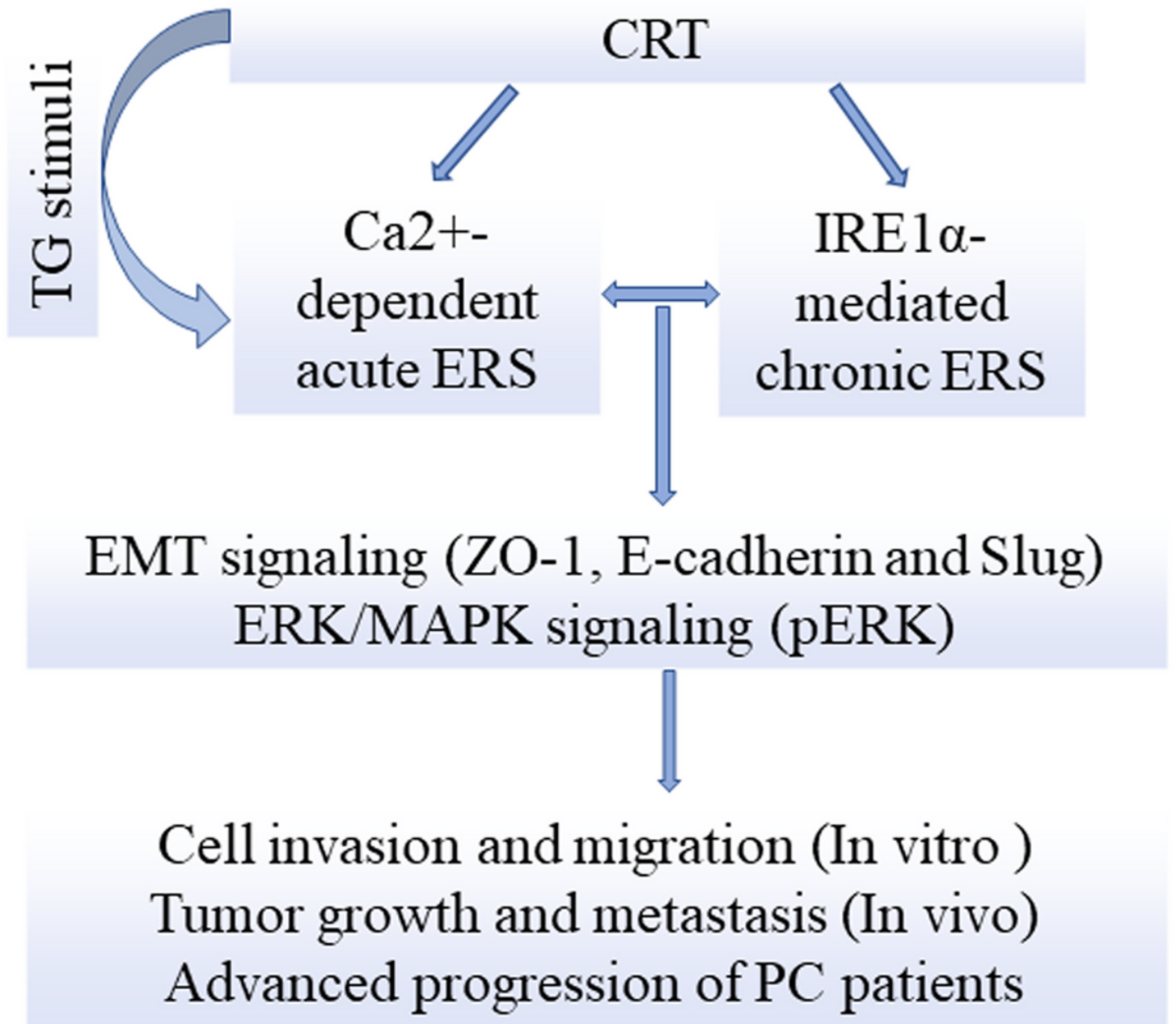


Figure 9

Calreticulin promotes EMT in pancreatic cancer via mediating Ca²⁺ dependent acute and chronic endoplasmic reticulum stress.

Supplementary Files

This is a list of supplementary files associated with this preprint. Click to download.

- [SupplementalMaterialFigure1.tif](#)
- [SupplementalMaterialFigure2.tif](#)
- [SupplementalMaterialFigure3.tif](#)